Global Journal of Environmental Science and Management
(GJESM)

Homepage: https://www.gjesm.net/

Podcasts

ORIGINAL RESEARCH PAPER

Hydrodynamic simulation experiment of tidal pump in strait waters

W.S. Pranowo[1,2,3,*], K. Malik[1,4], D. Adrianto[1,4], A. Kurniawan[1,5]

[1] *Study Program of Oceanography, Indonesian Naval Postgraduate Military Service School (STTAL), West Kelapa Gading, Jakarta, Indonesia*

[2] *Research Center for Climate and Atmosphere (BRIN), B.J. Habibie Science and Technological Park, South Tangerang City, Banten, Indonesia*

[3] *Korea-Indonesia Marine Technology Cooperation and Research Center, Jakarta, Indonesia*

[4] *Hydro-Oceanography Center, Indonesian Navy, Jl. Pantai Kuta V/1, East Ancol, North Jakarta, Indonesia*

[5] *Faculty of Geography, Universitas Gadjah Mada, Jl. Kaliurang, Sekip Utara, Bulaksumur Sinduadi Sleman, Yogyakarta, Indonesia*

ARTICLE INFO

Article History:
Received 05 September 2024
Revised 09 December 2024
Accepted 13 January 2025

Keywords:
Bangka Strait
Downwelling
Numerical model
Tidal pump
Upwelling

ABSTRACT

BACKGROUND AND OBJECTIVES: Tidal phenomena, characterized by the rise and fall of sea surface levels, play a critical role in marine dynamics, including the formation of upwelling and downwelling currents. These currents significantly influence nutrient distribution and material exchange in coastal waters. The objective of this study is to analyze the vertical current movements generated by tidal pumping in the Bangka Strait, with a particular focus on their association with tidal asymmetry and changes in the underwater topography.

METHODS: A numerical simulation approach was employed using the Mike 3 Flexible Mesh software to model the hydrodynamics of the Bangka Strait. The input data included tidal measurements from the Geospatial Information Agency and bathymetric data from the Indonesian Navy Hydro-Oceanography Center. Over a duration of nine days, the simulation examined tidal patterns and their role in influencing vertical currents. Statistical methods were employed to validate the model, demonstrating a significant correlation and negligible errors when comparing simulation results and field data.

FINDINGS: The study revealed that during high tide, upward currents (upwelling) were observed with speeds ranging from 0.0005 to 0.0016 meters per second, while during low tide, downward currents (downwelling) occurred with speeds 0.0002 to 0.0035 meters per second. Significant alterations in vertical current direction were observed due to bathymetric changes, particularly within the depth range of 2 to 6 meters. There was a clear indication of tidal asymmetry, with the northern Bangka Strait exhibiting a tidal range of 3.8 meters, while the southern region recorded a range of 2 meters. These variations influenced vertical current speeds and nutrient distribution patterns. This study demonstrated that the K_1 amplitude exhibited the most pronounced increase during a supermoon event, pointing to a likely strong correlation.

CONCLUSION: The findings demonstrate the significant role of tidal pumping in shaping the hydrodynamics of the Bangka Strait, with implications for nutrient mixing and material transport. The outcomes yield significant information that can aid in the stewardship of coastal resources and the advancement of sustainable infrastructure in marine ecosystems. This study underscores the importance of numerical modeling in understanding complex marine dynamics and highlights the need for continued research to address the ecological and environmental impacts of tidal-induced currents.

DOI: 10.22034/gjesm.2025.02.13

This is an open access article under the CC BY license (http://creativecommons.org/licenses/by/4.0/).





NUMBER OF REFERENCES
63



NUMBER OF FIGURES
9



NUMBER OF TABLES
5

*Corresponding Author:
Email: *widodo.setiyo.pranowo@gmail.com*
Phone: +62821 1163 7144
ORCID: 0000-0002-5798-4181

Note: Discussion period for this manuscript open until July 1, 2025 on GJESM website at the "Show Article".

INTRODUCTION

Bangka Strait is geographically a narrow gap between Bangka Island and the eastern mainland of South Sumatra. The strait holds significant economic importance for South Sumatra and Bangka Island, serving as a gateway to the maritime world for both regions (Zubir, 2015; Kurniawan *et al*., 2021), and contributing to the progress of maritime activities in western Indonesia. Since the Srivijaya period, the Bangka Strait has played a vital role as a key shipping channel. Previous studies indicate that this route has played a significant role in fostering human interaction and the dissemination of culture, owing to its advantageous geographical position (Fauziyah *et al*., 2022). In addition to trade and economic activities, the strait has been observed to play an important role in mining, with Bangka Island being the largest offshore tin mining site in Indonesia (Pamungkas and Husrin, 2020). Recognizing the vital role of the Bangka Strait, it is imperative to develop a thorough knowledge of its hydrodynamic features (Ambalika *et al*., 2019; Fauziyah *et al*., 2022; Kusumawardani *et al*., 2024). The objective of this study is to utilize numerical modeling techniques to simulate the hydrodynamic conditions of the Bangka Strait. The simulation results are anticipated to provide insights into the past, present, and future conditions of the waters. The insights gained from these observations can be instrumental for port and water engineering projects, ensuring that developments associated with the sea do not compromise existing biological resources. Various marine dynamics phenomena, such as upwelling and downwelling, are produced by vertical current movements from the bottom to the surface or vice versa (Nakanowatari *et al*., 2021; Cheng *et al*., 2022). These currents are typically caused by wind pushing sea surface layer (Johnston and Colin 2022; Podymov *et al*., 2023), creating a void in the water mass above it (Trautman and Walter, 2021). Based on observation, upwelling and downwelling can also occur due to seabed topography and changes in the physical properties of seawater, including temperature, salinity, and density in the water column (Coogan *et al*., 2019; Lorente *et al*., 2020; He and Mahadevan, 2021; Johnston and Colin, 2022; Leclercq *et al*., 2024; Li *et al*., 2024). Moreover, it has been established that these currents may be impacted by tidal pumps in certain conditions and specific locations. Tidal movements, characterized by the cyclical rise and fall of sea levels, are driven by the gravitational forces exerted by the moon and sun, as well as the seabed's topographical characteristics (Sarkar *et al*., 2019; Huang and Li, 2024; Li *et al*., 2024; Zou *et al*., 2024). During these movements, tidal pump (Xiao *et al*., 2018; Wu, 2021), stirs nutrients (Liu *et al*., 2017; Zhao *et al*., 2023; Li *et al*., 2024), temperature, and salinity in the water column (Becherer *et al*., 2016; Stevens and Smith, 2016; Zhao *et al*., 2019; Du *et al*., 2022; Xu *et al*., 2023). The process occurs continuously during tidal phenomena, specifically in estuarine areas (Becherer *et al*., 2016). In stratified coastal waters, surface and bottom tidal currents rotate in opposite directions, resulting in upwelling on one side and downwelling on the other, depending on the current's orientation (Xu *et al*., 2023). In relatively narrow straits, the localized effects of tidal pumping significantly influence the broader dynamics within the strait region (Xiao *et al*., 2018; Zhou *et al*., 2020; Martín *et al*., 2023). Straits serve as key connectors between seas or oceans, where tidal differences on either side can generate strong currents, driving water movement (Cucco *et al*., 2016). This mechanism enables the movement of materials across the strait, encompassing sediments, nutrients, and potentially harmful pollutants (Fourniotis, 2024). The tidal pumping process in straits typically occurs when tidal height differences on either side create a pressure gradient strong enough to drive water through the strait (Børve *et al*., 2021; Hosseini *et al*., 2023). In instances of tidal asymmetry, where high tide is experienced on one side of the strait while the opposite side experiences low tide, water flows from the high-tide area to the low-tide area, carrying with it suspended particulate matter. As the tidal cycle progresses and the gradient reverses, the resulting bidirectional flow facilitates the exchange of water masses, enhancing nutrient redistribution and contributing to the dispersal of pollutants across broader spatial scales (Yin *et al*., 2022; Fu *et al*., 2023; Xu *et al*., 2023). This phenomenon plays a vital role in marine ecosystems and has important consequences for coastal water quality and human activities, including fisheries and maritime transportation. The ecological impacts of tidal pumping in straits vary widely, depending on the physical characteristics of the strait—such as depth, width, and seafloor topography—as well as the prevailing tidal conditions (Jeon *et al*., 2024). Under

particular circumstances, tidal pumping may increase biological productivity by transferring nutrients from the deep ocean to shallower coastal regions, which in turn supports the proliferation of phytoplankton and other marine organisms (Zhao *et al.*, 2019). However, in other straits, this phenomenon can contribute to the distribution of pollutants or hazardous materials, potentially harming local ecosystems and posing risks to human health (Zhao *et al.*, 2019). In areas near significant urban centers or industrial zones, tidal pumping can facilitate the movement of pollutants from sources of contamination to wider regions, thereby affecting water quality and marine ecosystems (Hananto and Prananda, 2020). Recent research on tidal pumping highlights the complexity of this phenomenon and underscores the importance of a deeper understanding for effective coastal resource management. Zhao *et al*. (2023) exploring the use of tidal pumping as a mechanism for alternative energy inputs, presenting promising opportunities for sustainable energy advancement and the optimization of coastal resources. Kersten *et al*. (2022) and Liu *et al*. (2017) state that tidal pumping is recognized as a primary driving force influencing water exchange between land and sea, biogeochemical reactions within tidal aquifers, and nutrient loading to the ocean. Understanding tidal pumping in straits is vital, especially considering the impacts of climate change, which can disrupt global tidal patterns and subsequently affect the mechanisms of tidal pumping. Sea-level rise and climate change may reshape the physical characteristics of straits, such as their width and depth, potentially modifying the intensity and impacts of tidal pumping. Consequently, additional research is essential to forecast the future development of this phenomenon and to determine how coastal resource management can be modified to respond to these changes. Overall, tidal pumping in straits is a complex and dynamic process with significant implications for marine ecosystems and human activities in coastal areas. Recent studies have provided valuable insights into its mechanisms and impacts, but much remains to be learned to ensure that coastal management can accommodate ongoing environmental changes. To protect sensitive ecosystems and promote the sustainable use of marine resources in the future, it is vital to adopt a more integrative and science-driven approach to the management of straits and coastal areas. Given the strategic position of the Bangka Strait as a transportation corridor and an ecological migration route. This study aims to examine and analyze the occurrence of upwelling and downwelling phenomena induced by tidal pump in Bangka Strait in Indonesia using the Mike 3 FM numerical modeling software in 2022. The data used include depth, and water level condition along boundary of Bangka Strait of Indonesia.

MATERIALS AND METHODS

The input used for the boundary model area comprised tidal data from the geospatial information agency or badan informasi geospasial (BIG), with measurements from Muntok Station in the north at 2° 5’ 5.64” south (S) - 105° 7’ 58.8” east (E) and Sadai Station in the south at 3° 0’ 51.48” S - 106° 26’ 49.2” E). The model simulation lasted for 1 hour (h) each day from July 18 to July 26, 2022. This date range was selected as it corresponds with the supermoon event that peaks during the eastern season in July 2022. It is also important to state that bathymetry data comprised digitization from nautical chart number 104 of the Indonesian Navy Hydro-Oceanography Center (Pushidrosal), which had a scale of 1:500.000. The analysis excludes various external influences, such as wind and the contribution of freshwater from river mouths, concentrating instead on the principles of barotropic modeling as outlined by (Ding *et al.*, 2012; Nugroho *et al.*, 2018; Ajiwibowo and Pratama, 2022). Fig. 1 presents a graphical representation of the research flowchart.

The present study included the use of a quantitative method with mathematical equations and the proposed model was validated using statistical analysis, which comprised tables, graphs, images, and diagrams. The configuration of the model design employed during the exploration is detailed in Table 1.

The model domain utilizes a flexible mesh, with the mesh formation criteria detailed in Table 2. Following this, depth interpolation was conducted utilizing the digitized Indonesian Nautical chart, employing the Natural Neighbor method.

Throughout this research, the simulation outcomes were analyzed both horizontally and vertically to assess the existing conditions within the water column. The three-dimensional model simulation divided the current into three components,

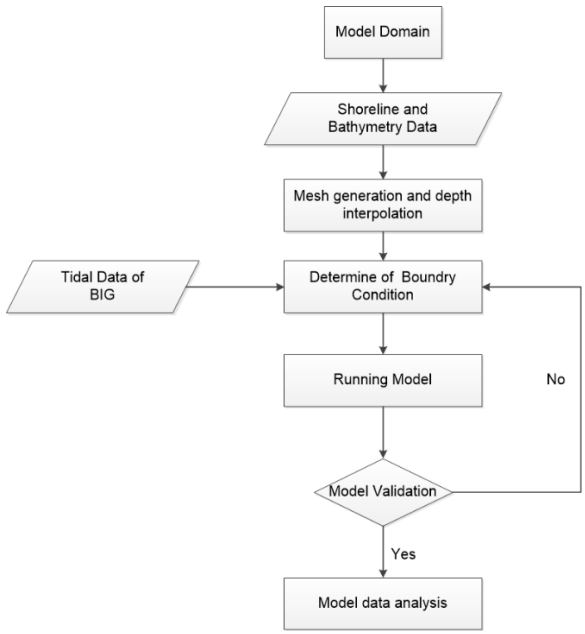

Fig. 1: The study flowchart

Table 1: Model design configuration

Parameter	Description
Simulation period	18/07/2022 – 26/07/2022
Time interval	3600 second
Number of time intervals	192
Horizontal eddy viscosity	Smagorinsky formulation
Vertikal eddy viscosity	Log law formulation
Bed resistance	Roughness height

Table 2: Mesh formation criteria in the model area

No.	Mesh	Description
1	Maximum elements	$2x10^{-3}$ deg^2. ($degree^2$)
2	Smallest angle	26°
3	Number of elements	14751
4	Number of points	7959

namely u and v representing horizontal currents as well as w representing vertical currents. In line with prior studies, a positive vertical velocity (w) suggests that the current is moving upward, a phenomenon termed upwelling. In contrast, a negative vertical velocity indicates a downward current, commonly referred to as downwelling (Mustikasari *et al*., 2015). Accordingly, the developed model overlaid the surface hydrodynamic phenomenon with w velocity value to examine the upwelling or downwelling phenomena in Bangka Strait. The design of the vertical cross-section was executed along the Bangka Strait, as indicated by the coordinates detailed in Table 3.

Study location including mesh formation, depth interpolation results, tidal station positions as validation of the model results, are shown in Fig. 2. The model was developed using the three-dimensional incompressible Reynolds average Navier

Table 3: Vertical profile coordinate of Bangka Strait

Point	Longitude	Latitude
1	104.9602	-2.01337
2	105.3421	-2.27635
3	105.6834	-2.32331
4	105.9025	-2.8524
5	106.2031	-3.00894

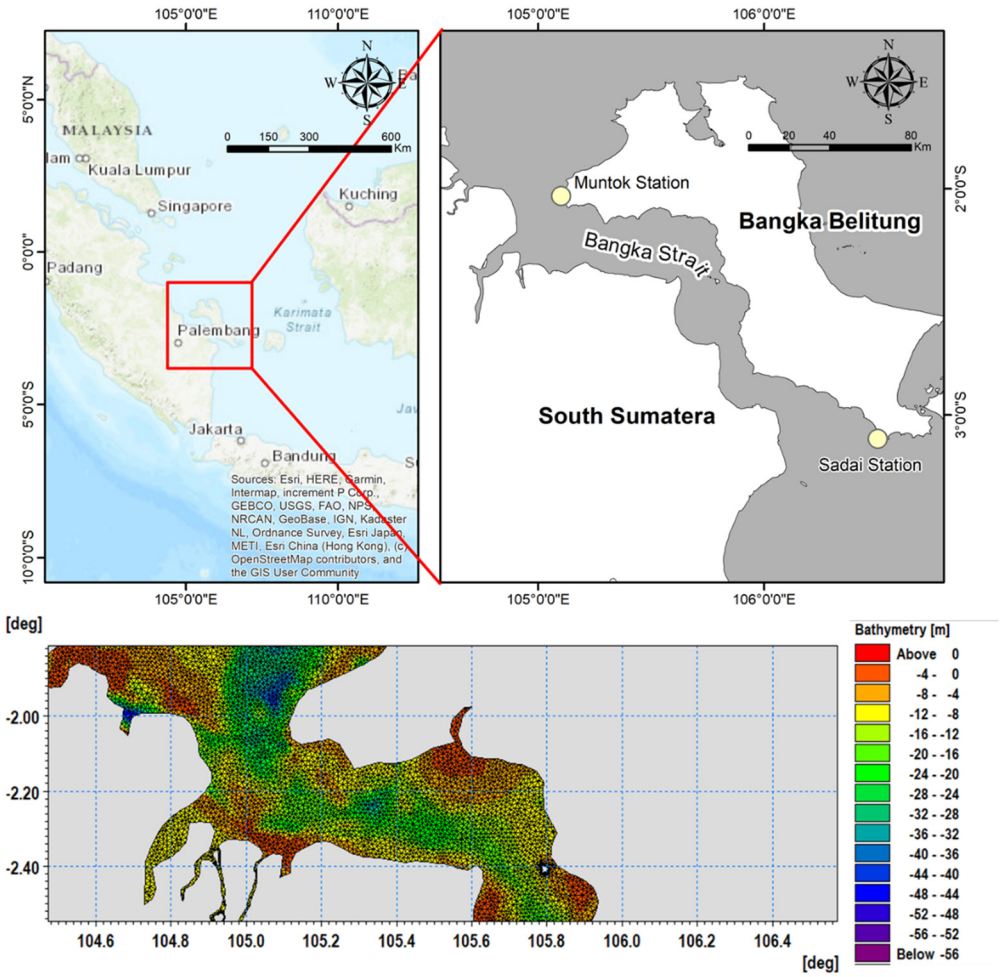

Fig. 2: Geographic location of the study araea in Bangka Strait of Indonesia, along with the mesh formation, depth interpolation results, validation tidal station positions

Stoke equation with the assumption of Boussinesq and hydrostatic pressure (Yasra *et al*., 2022). A three-dimensional numerical strategy was employed for the preparation, integrating the sigma and Z-level systems to maintain velocity at the water's bottom. Within the realm of oceanography, the sigma system serves as a discretization framework used in deep waters, facilitating the conversion of depth changes into the bottom layer by "stretching" vertical domain (Zamani and Koch, 2020). Furthermore, to obtain higher geometric resolution along the complex coastline, the unstructured grid was applied

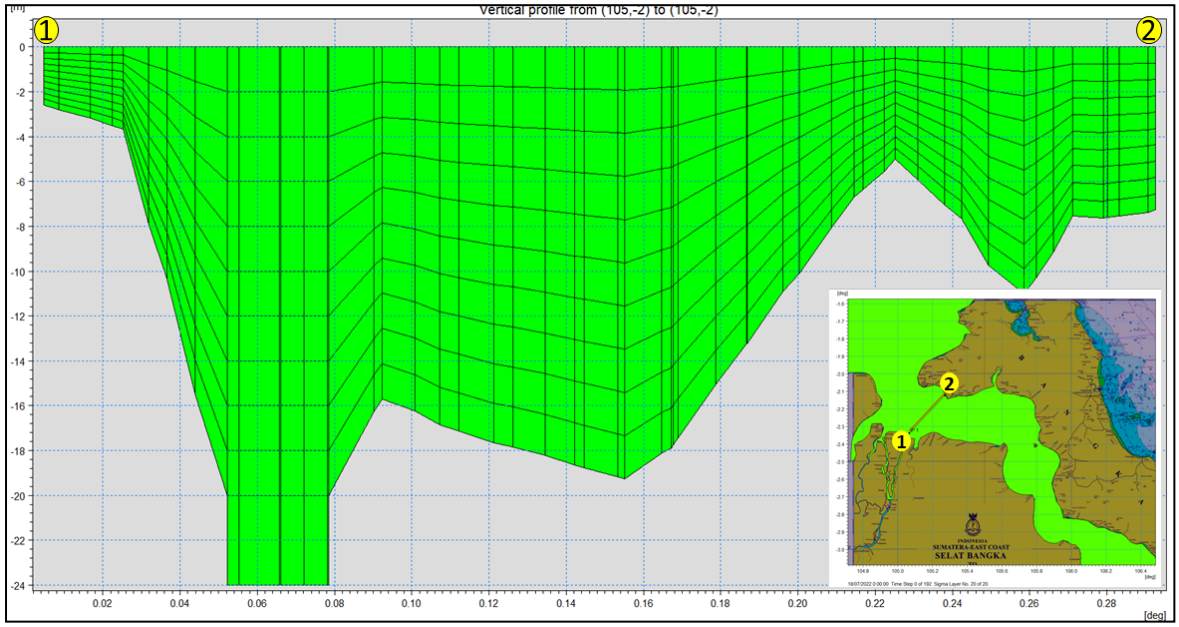

Fig. 3: Vertical cross-section of the combined sigma and Z-level methods (hybrid)

horizontally. This enabled the entire research area to be approached in accordance with actual conditions. This study implemented a vertical mesh that combined the sigma and Z-level coordinate systems, organized according to an equidistant framework. It is also important to state that the surface, to a depth of 20 meters (m) used the sigma method, while the rest utilized Z-level method with a grid spacing of 4 m as shown in Fig. 3. The formulation of Continuity in Cartesian plane can be used as Eq. 1 (DHI 2017):

$$\frac{\partial u}{\partial x}+\frac{\partial v}{\partial y}+\frac{\partial w}{\partial z}=0 \tag{1}$$

Meanwhile, the momentum equations on the x, y, and z axes can be shown as Eqs. 2, 3 and 4 (DHI, 2017):

$$\frac{\partial u}{\partial t}+\frac{\partial u^2}{\partial x}+\frac{\partial vu}{\partial y}+\frac{\partial wu}{\partial z}= fv-\frac{1}{\rho_0}\frac{\partial q}{\partial x}-g\frac{\partial \eta}{\partial x}-\frac{1}{\rho_0}\frac{\partial p_a}{\partial x}- \frac{g}{\rho_0}\int_z^\eta \frac{\partial \rho}{\partial x}+F_u-F_{vx}+\frac{\partial}{\partial z}\left(v_t^v\frac{\partial u}{\partial z}\right) \tag{2}$$

$$\frac{\partial v}{\partial t}+\frac{\partial uv}{\partial x}+\frac{\partial v^2}{\partial y}+\frac{\partial wv}{\partial z}= -fu-\frac{1}{\rho_0}\frac{\partial q}{\partial y}-g\frac{\partial \eta}{\partial y}-\frac{1}{\rho_0}\frac{\partial p_a}{\partial y}- \frac{g}{\rho_0}\int_z^\eta \frac{\partial \rho}{\partial y}+F_v-F_{vy}+\frac{\partial}{\partial z}\left(v_t^v\frac{\partial v}{\partial z}\right) \tag{3}$$

$$\frac{\partial w}{\partial t}+\frac{\partial uw}{\partial x}+\frac{\partial vw}{\partial y}+\frac{\partial w^2}{\partial z}= -\frac{1}{\rho_0}\frac{\partial q}{\partial z}+F_w-F_{vz}+\frac{\partial}{\partial z}\left(v_t^v\frac{\partial w}{\partial z}\right) \tag{4}$$

Where, t is time, x, y, and z are Cartesian coordinates, η represents surface elevation, u is the x-axis velocity component, v denotes the y-axis velocity component, w is the z-axis velocity component, and f is Coriolis parameter with $f=2\Omega\sin\phi$ (Ω is the angle of revolution and ϕ is the geographic latitude). Furthermore, other parameters of the equation include v_t^v, which represents vertical eddy viscosity, g, the acceleration due to gravity, p_a atmospheric pressure on the surface, ρ water density, ρ_0 reference density and F, horizontal

diffusion. The sigma method on vertical plane of the S coordinate discretization was in accordance with formation by Song and Haidvogel (1994), where the first vertical equidistant discretization (-1≤ s ≤ 0) was applied, using Eq. 5 (Song and Haidvogel, 1994):

$$S_i = -\frac{N_\sigma + 1 - i}{N_\sigma} \quad \text{with } i = 1,(N_\sigma + 1) \tag{5}$$

The sigma coordinate system formulation is discretized, using Eqs. 6 and 7 (Song and Haidvogel, 1994):

$$\sigma_i = 1 + \sigma_c S_i + (1 - \sigma_c) C(S_i) \text{ with } i = 1,(N_\sigma + 1) \tag{6}$$

Where :

$$C(S) = (1-b)\frac{\sin(\Theta_s)}{\sin(\Theta)} + b\frac{\tanh\left(\Theta\left(s+\frac{1}{2}\right)\right) - \tanh\left(\frac{\Theta}{2}\right)}{2\tanh\left(\frac{\Theta}{2}\right)} \tag{7}$$

Where; σc is a weighting factor between the equidistant distribution and the strain formulation (0 < σc ≤ 1), with 1 showing an equidistant distribution and 0 showing a strain distribution. Furthermore, Θ is the surface control parameter (0 < θ ≤ 20), and b represents the basic control parameter (0 ≤ b ≤ 1).

Model validation

Following the successful execution of a model simulation, validation was carried out to evaluate the discrepancies between the model outcomes and the field data. Model validation incorporated several statistical formulations, all of which were used to evaluate the model results. The main statistical metric employed is the root mean square error (RMSE). This measure is commonly utilized to assess the precision of predictive data. In general, a prediction is considered close to accurate when RMSE value approaches zero, with a maximum tolerated limit of 0.4 for the model to be accepted. This formulation is widely regarded as an excellent tool for determining the level of error in modeling. RMSE value was calculated using Eq. 8 (Neill and Hashemi 2018):

$$RMSE = \sqrt{\frac{1}{N}\sum_{i=1}^{N}(M_i - O_i)^2} \tag{8}$$

Once RMSE was determined, the Pearson correlation coefficient was utilized to analyze the relationship between the model results and the field data, allowing for an assessment of the correlation's strength (Smith, 2021). Generally, Pearson correlation is calculated using Eq. 9 (Smith, 2021):

$$r = \frac{n\sum xy - (\sum x)(\sum y)}{\sqrt{\left(n\sum x^2 - (\sum x)^2\right)\left(n\sum y^2 - (\sum y)^2\right)}} \tag{9}$$

Table 4 presents the obtained results on the correlation between coefficients and relationship levels in the Pearson correlation method (Malik *et al.* 2023).

RESULTS AND DISCUSSION

Validation results

Results from the simulation demonstrate that the validation of surface elevation at the Muntok Station, in comparison to field data, achieved RMSE and correlation values of 0.17 and 0.98 respectively. The overlay between the model results graph and field data is shown in Fig. 4.

The validation results of the model's surface elevation at Sadai Station position with field data showed an RMSE value of 0.04 with a correlation value of 0.99. The overlay graph presented in Fig. 5 depicts the relationship between the surface elevation of the simulation results and the corresponding field data.

The validation results from both tidal observation stations show that the model performed well, as shown by the very small RMSE values below 0.4 and correlation values above 0.80, which reflects a strong correlation between the simulation results and field

Table 4: Pearson correlation table

Coefficient interval	Relationship level
0.00 – 0.199	Very low
0.20 – 0.399	Low
0.40 – 0.599	Moderate
0.60 – 0.799	Strong
0.80 – 1.000	Very strong

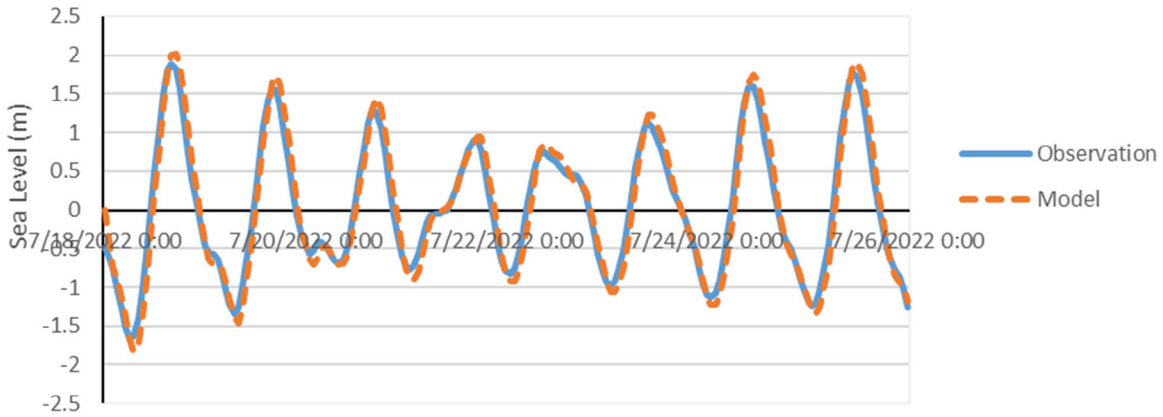

Fig. 4: Graph of field and model tidal validation at Muntok Station

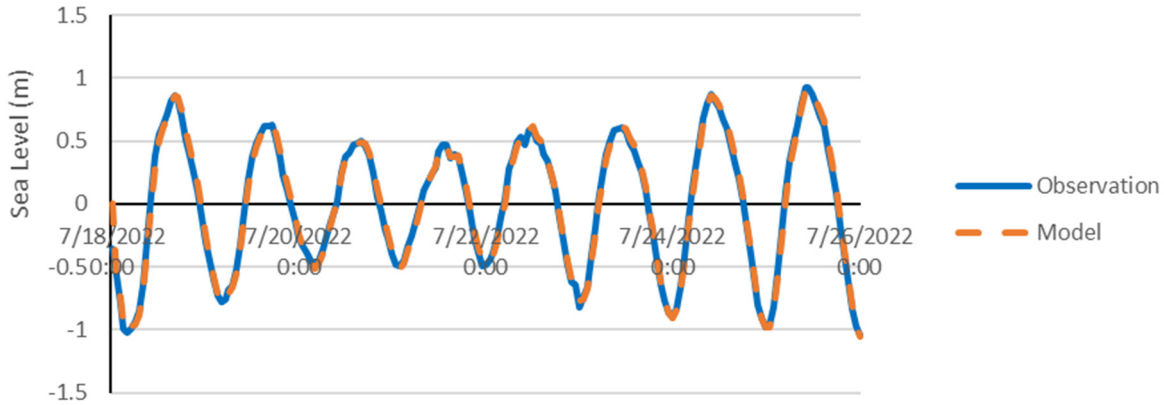

Fig. 5: Graph of field and model tidal validation at Sadai Station

data. The observations led to the conclusion that the results from the model simulation were appropriate for subsequent analysis. Surface elevation data from the model results at the two tidal stations, Muntok and Sadai, were used to perform harmonic component calculations adopting Within the Mike software, the Tide Analysis of Height tool is grounded in the least squares principle for its calculations. The tidal harmonic constants at Muntok and Sadai Stations are shown in Tables 5 and 6 respectively**.** Findings from the tidal harmonic constants at both stations reveal that K1 was the most prominent among the various constants. Qualitatively, this is in line with Hatayama *et al.* (1996) who stated that tidal propagation in the western Indonesian waters showed the K1 component to be more dominant than M2 component. The prevailing influence was linked to the tidal propagation emanating from the Pacific Ocean. Vertically, the movement of surface elevation along Bangka Strait, according to the vertical profile coordinate listed in Table 3 , shows that when approaching high tide, the surface elevation moves from the north and south of the strait towards the middle. As low tide approaches, the water begins to flow from the center of the strait, subsequently moving back toward both the northern and southern ends, as illustrated in Fig. 6.

The obtained results are also in line with Hatayama *et al.* (1996), where tidal propagation was described based on the constant K1 in Indonesian waters in Bangka Strait. This area serves as a junction for tidal flows originating from the Malacca Strait and the

Table 5: Tidal harmonic constants from the model results

No.	Muntok station			Sadai station	
	Name	Amp (m)	Phase (deg.)	Amp (m)	Phase (deg.)
1	Z0	0.0325	0	0.0096	0
2	K1	0.9166	61.48	0.5676	44.54
3	M2	0.3506	11.85	0.0751	293.44
4	M3	0.0244	313.29	0.0048	247.86
5	M4	0.0222	32.25	0.0105	92.14
6	2MK5	0.0198	40.69	0.0199	53.15
7	2SK5	0.0073	215.06	0.0006	337.9
8	M6	0.0051	358.19	0.0057	51.64
9	3MK7	0.0083	247.3	0.0043	209.82
10	M8	0.0118	349.66	0.0061	322.88

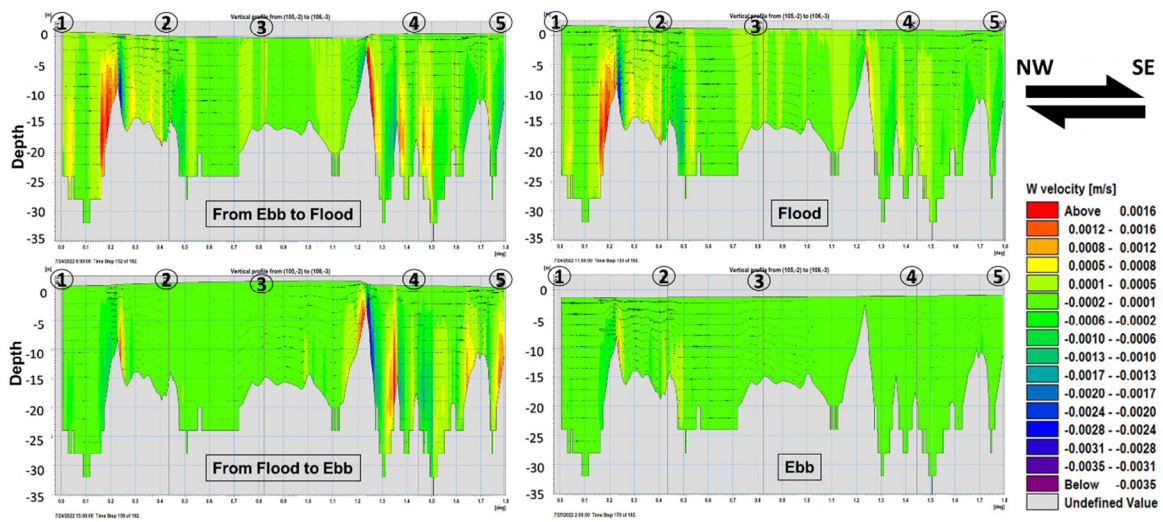

Fig 6: The surface elevation pattern movement along Bangka Strait based on Table 3 coordinate

South China Sea to the north, as well as the Java Sea in the south. Tidal propagation scheme in Indonesian waters is shown in Fig. 7.

Surface current circulation and vertical current

The surface current derived from the model simulation results exhibits a pattern consistent with the propagation of high water. As high tide approaches, the current is noted to flow into the strait's mouth from both the northern and eastern directions, converging at the center. Meanwhile, when approaching low tide, the current moved from the middle of the strait to the north and south, as shown in Fig. 8a and b. Fig. 8a and b show the color gradation represents w velocity component, with positive and negative w velocity values showing upwelling and downwelling respectively. Fig. 8, when viewed horizontally, shows that as high tide was approached, the area in the north of the strait with a w velocity above 0.00016 meter per second (m/s) became greater compared to the south. This condition indicates that the northern region of the strait underwent a significant upwelling phenomenon. Meanwhile, as low tide approaches, w velocity values in both the north and south tend to be homogeneous, around -0.00004 m/s, showiing downwelling currents.

Findings from the horizontal simulation reveal that with the approach of high tide, the W velocity value in the northern part of the strait is higher than that in the southern part (Fig. 8). This difference in W velocity was probably due to the varying water levels between the north and south of the strait. Tidal range

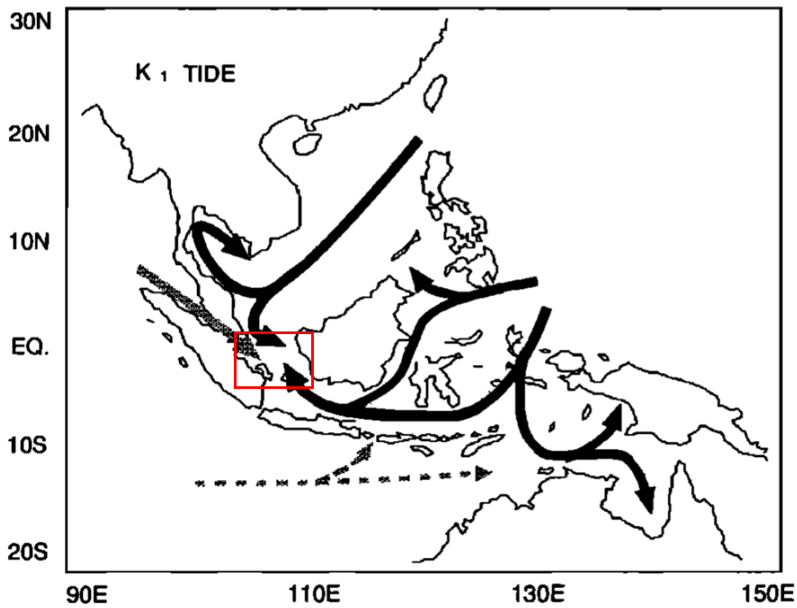

Fig 7: Tidal propagation scheme due to constant K1 in Indonesian waters, and red box is domain of the study (Hatayama *et al.*, 1996)

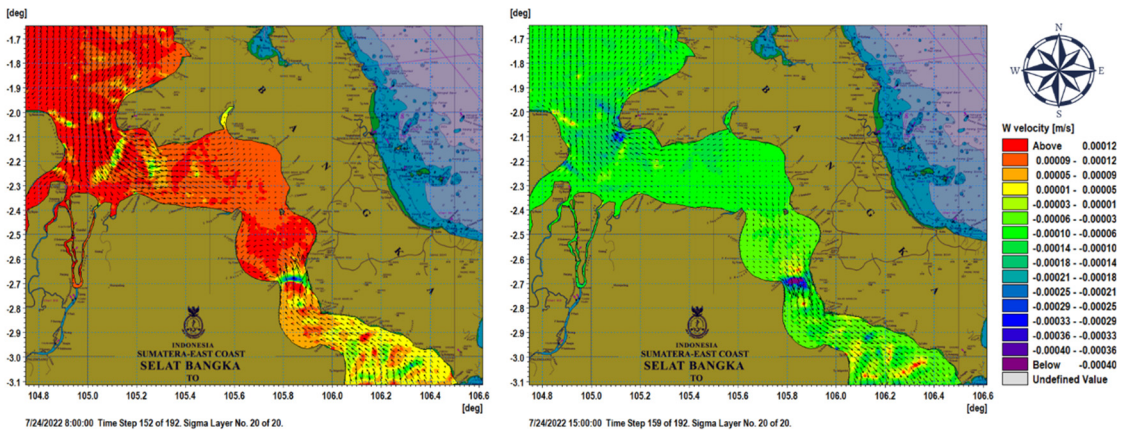

Fig. 8: Surface current pattern when approaching high tide (8a) and Surface current pattern when approaching low tide (8b)

in the north was approximately 3.8 m, while that of the south was only 2 m, as shown in Fig. 9.

The results obtained from the model simulation were analyzed vertically by cutting Bangka Strait following the coordinates and the scheme shown in Fig. 2, with the conditions presented in Fig. 6. As high tide was approached, the surface elevation at points 1, 2, and 3, points 4 and 5 of Bangka Strait was already at high tide. The vector W, extending from point 1 to point 2, demonstrated upwelling, but at depths of 6 and 2 m, it deflected downward. The current vector w between points 2 and 3 showed similar upward movement, which also deflected at depths of 6 and 2 m. With the arrival of low tide in the northern region (point 1) and southern areas (points 4 and 5) of the Bangka Strait, the surface elevation had dropped to low tide. In contrast, points 2 and 3 continued to experience high tide conditions. The current vector

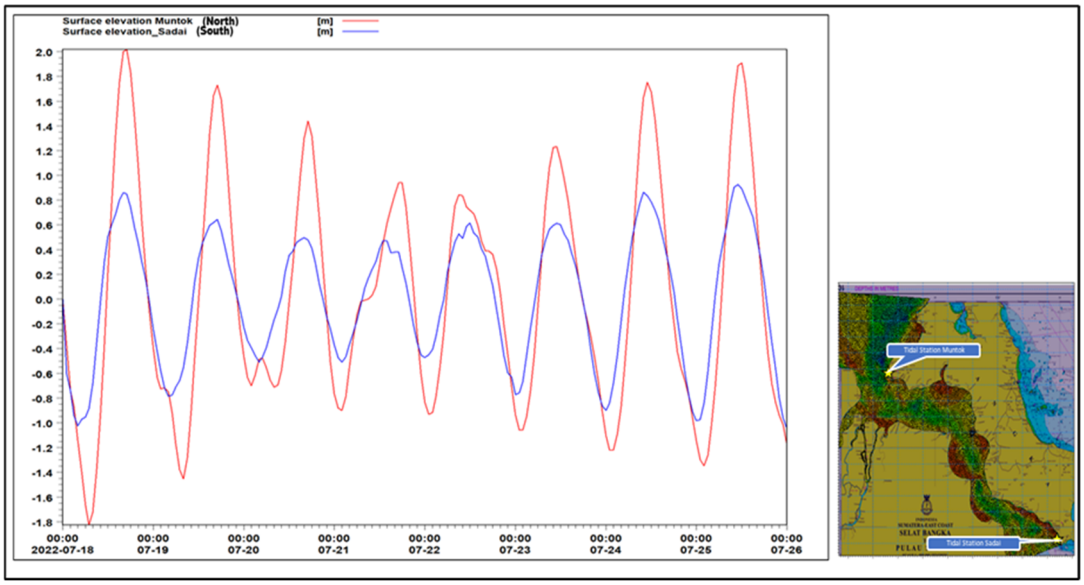

Fig. 9: The difference in tidal elevation between north and south stations

W from points 1 to 2 showed downwelling, with upward deflection at depths of 6 and 2 m. Between points 2 and 3, the current vector w also showed downwelling, which subsequently experienced upwelling deflection at the same depths. Overall, the findings from the model simulation demonstrated that the W component vector's movement in the water column conformed to a tidal pattern, observed in both horizontal and vertical dimensions. This was evidenced by the fact that as high tide was approached, w component vector moved upward, but as low tide was approached, it moved downward. Furthermore, the simulation revealed that variations in underwater topography affected the dynamics of upwelling and downwelling, aligning with the research conducted by. Sabhan *et al.* (2020). Topographic variations (e.g. sills) make a significant contribution to the formation of upward vertical currents (pumping/upward velocity), especially in the near-surface area seen in Fig. 6, and the results of this study are similar to those presented by Pranowo *et al.* (2014) and Nugroho *et al.*, (2018). Upwelling speed obtained from the simulation in Bangka Strait was observed to be between the range from 0.0005 to 0.0016 m/s, while downwelling speed ranged from 0.0002 to 0.0035 m/s presented in Fig. 6. These values were smaller than those reported by Pranowo *et al.* (2014) who examined Bone Bay waters in August 2004. During the investigation, Pranowo *et al.* (2014) stated that the upwelling speed value in Bone Bay area ranged from 0.0005 - 0.0035 m/s, while downwelling speed was between the range from 0.0005 - 0.0046 m/s. In similar aquatic environments, particularly the Ombai Strait, the documented vertical current velocity values appear to be marginally greater, attaining a maximum of 0.00076 m/s (Kurniawan *et al.*, 2023). Most tidal pump and upwelling experiments are currently conducted in estuarine areas or nearshore waters (Yu *et al.*, 2014; Ajiwibowo and Pratama, 2022; Du *et al.*, 2022; Zhao *et al.*, 2023) or laboratory-based experiments (Xiao *et al.*, 2018; Rahuna *et al.*, 2023). Only a small number of experiments have ever been recorded in the waters of the strait (Sánchez-Garrido *et al.*, 2015; Gonzalez *et al.*, 2023), and the main focus of several vertical current velocity experiments is the development of renewable energy (Calero *et al.*, 2014; Orhan and Mayerle, 2020; Hazim *et al.*, 2021; Ajiwibowo and Pratama, 2022). It is crucial to highlight that, apart from the differences in research sites between the strait and the bay, the discrepancies in results may also stem from the varying depths present in both areas. The Bangka Strait was found to have a depth of approximately ~30 m, in contrast to Bone Bay, which reached around 400 meters.

Nevertheless, research by Mustikasari *et al.* (2015), which simulated currents across all Indonesian waters over a one-year period, indicated that the upwelling speed during the East season (August) in Bangka Strait ranged of $5x10^{-6}$ – $2x10^{-5}$ m/s. It appears that this study produces higher upwelling speed, which is thought to be related to the different resolutions of the applied models. In general, this study uses a more detailed unstructured grid with more specific locations, so that the bottom topography of the waters can be better replicated. Hatayama *et al.* (1996) indicate that the tidal behavior in the Bangka Strait is shaped by interactions from surrounding regions, with the K_1 tide mainly resulting from tidal forces that come from the Pacific, in contrast to the M_2 tide, which is affected by inputs from both the Pacific and Indian Oceans. This regional variability underscores the role of tidal forcing from the Malacca Strait, South China Sea, and Java Sea in determining tidal stability and predictability. Under changing climate conditions, shifts in ocean circulation and sea-level rise could alter the dominance of Pacific or Indian-origin tidal forces, impacting the long-term behavior of tidal currents in the Bangka Strait. Comprehending these regional factors is important for predicting future tidal dynamics in this area. The study demonstrated that during a supermoon event, the K_1 amplitude had the most considerable increase, suggesting a robust potential correlation. This contrasts with the findings of Tiatama *et al.* (2024) in the waters of Semarang Bay (northern coast of Java), which stated that the 2022 supermoon phenomenon does not directly influence K_1 tidal components. In certain cases, K_1 refers to a tidal constant used in sea-level calculations, which is influenced by the gravitational forces of the Moon and the Sun on Earth. The tidal pumping phenomena observed in this study have potential long-term ecological and environmental implications in strait ecosystems for futher research. By improving the vertical mixing of water bodies, tidal pumping aids in the transfer of nutrients from the benthic zone to the photic zone, which in turn supports primary productivity and encourages biodiversity. However, it also poses potential risks, such as increased turbidity that may hinder photosynthesis, and the redistribution of pollutants like heavy metals and microplastics, which can disrupt food webs and ecosystem dynamics. Additionally, tidal pumping influences oxygen levels in the water column, potentially leading to hypoxic conditions in poorly ventilated areas. These diverse effects emphasize the importance of conducting further studies to measure the long-term implications and shape conservation strategies, particularly in light of shifting environmental circumstances and escalating anthropogenic pressures.

CONCLUSION

This study successfully validated the hydrodynamic simulation model for the Bangka Strait using tidal data from Muntok and Sadai Stations. The model recorded root mean square error values of 0.17 and 0.04, and correlation coefficients of 0.98 and 0.99, which signify a robust alignment with field data. These validation results confirm the robustness and reliability of the simulation in capturing the tidal dynamics of the Bangka Strait. The findings demonstrated that tidal pumping within the Bangka Strait is heavily influenced by the asymmetry of tides and changes in bathymetric variations. Tidal range differences, with 3.8 meters in the north and 2 meters in the south, created distinct patterns in vertical current dynamics. Upwelling was dominant during high tide, with velocities ranging from 0.0005 to 0.0016 meters per second, particularly in the northern region of the strait. In contrast, downwelling took place during low tide, exhibiting velocities ranging from 0.0002 to 0.0035 meters per second. Bathymetric topography significantly influenced vertical currents, particularly at depths between 2 and 6 meters, where changes in seabed slope caused deflections in current direction. Surface elevation patterns demonstrated a bidirectional flow, showing that water converges at the midpoint of the strait during high tide and spreads out to the north and south during low tide. The dominance of the K1 tidal harmonic constant in the Bangka Strait aligns with previous research on tidal propagation in Indonesian waters. The findings of this study indicated that the K_1 amplitude showed a significant increase during a supermoon event, suggesting a probable strong correlation. This highlights the significant contribution of tidal forces from the Pacific Ocean and the confluence of tidal movements from the Malacca Strait, South China Sea, and Java Sea. These interactions play a critical role in shaping the hydrodynamic characteristics of the Bangka Strait. In conclusion, this study provides valuable insights into the hydrodynamics of the Bangka Strait,

emphasizing the role of tidal pumping in influencing vertical currents and water column mixing. These results carry important practical consequences for the management of coastal resources, maritime navigation practices, and the preservation of ecosystems. Further research is recommended to explore seasonal variations, sediment transport, and the broader ecological impacts of tidal dynamics in this region.

AUTHOR CONTRIBUTIONS

W.S. Pranowo, the corresponding author, has main contributor with conceptualization, methodology, software, interpreted the results, formal analysis, data curation, writing - original draft preparation, visualization. K. Malik has contribute to data curation, methodology, software, formal analysis, writing - original draft preparation, visualization. D. Adrianto has contribute to investigation, resources, supervision, writing - review and editing. A. Kurniawan has contribute to visualization, validation, formal analysis, dan software.

ACKNOWLEDGEMENT

Tide data were obtained from BIG. Bathymetry data were obtained from Hydro-Oceanography Center (Pushidrosal). Modeling was conducted at the Hydro-Oceanography Laboratory, Indonesian Naval Postgraduate School (STTAL) in North Jakarta. Part of the analysis was conducted at the Climate and Atmospheric Research Center, National Research and Innovation Agency (BRIN).

CONFLICT OF INTEREST

The authors declare that there is no conflict of interests regarding the publication of this manuscript. In addition, the ethical issues, including plagiarism, informed consent, misconduct, data fabrication and/or falsification, double publication and/or submission, and redundancy have been completely observed by the authors.

OPEN ACCESS

©2025 The author(s). This article is licensed under a Creative Commons Attribution 4.0 International License, which permits use, sharing, adaptation, distribution and reproduction in any medium or format, as long as you give appropriate credit to the original author(s) and the source, provide a link to the Creative Commons license, and indicate if changes were made. The images or other third-party material in this article are included in the article's Creative Commons license, unless indicated otherwise in a credit line to the material. If material is not included in the article's Creative Commons license and your intended use is not permitted by statutory regulation or exceeds the permitted use, you will need to obtain permission directly from the copyright holder. To view a copy of this license, visit: http://creativecommons.org/licenses/by/4.0/

PUBLISHER'S NOTE

GJESM Publisher remains neutral with regard to jurisdictional claims in published maps and institutional afflictions.

ABBREVIATIONS

^{o}	Degree
$'$	Minue
$''$	Second
BIG	Badan informasi geospasial
Deg.	Degree
E	East
F	horizontal diffusion
f	Coriolis parameter
h	Hour
M	Model result data
m	Meters
m/s	meter per second
n	Number of data pairs X and Y
O	Field data (BIG data)
RMSE	Root mean square error
S	South
t	time
u	x-axis velocity component
v	y-axis velocity component
W	vertical velocity

η	surface elevation
g	acceleration due to gravity
Ω	angle of revolution
p_a	atmospheric pressure
ϕ	geographic latitude
ρ	water density
ρ_0	reference density
ν_t^v	vertical eddy viscosity
Σx	Total number of variables X
Σy	Total number of variables Y
Σx^2	Square of total number of variables X
Σy^2	Square of total number of variables Y
Σxy	Multiplication result of total number of variables X and Y

REFERENCES

Ajiwibowo; H.; Pratama, M. B., (2022). Hydrodynamic model and tidal current energy potential in Lepar Strait, Indonesia. Int. J. Renew. Energy Dev., 11(1): 15–25 **(11 pages)**.

Ambalika, I.; Irma, A.; Aditya, P.; Mohammad, N.; Umroh, (2019). Oceanography database development in Bangka Seas. Adv. Eng. Res., 167: 22-26 **(5 pages).**

Becherer; Johannes; Götz, F.; Lars, U.; Hans, B., (2016). Estuarine circulation versus tidal pumping: Sediment Transport in a well-mixed tidal inlet. J. Geophys. Res. Ocean., 121(8): 6251–6270 **(20 pages).**

Børve, E.; Päl, E.I.; Ole, A.N., (2021). Rectified tidal transport in lofoten-vesterälen, Northern Norway. Ocean Sci., 17(6): 1753–1773 **(21 pages).**

Calero Quesada; M. C.; García Lafuente, J.; Sánchez Garrido, J. C.; Sammartino, S.; Delgado, J., (2014). Energy of marine currents in the Strait of Gibraltar and its potential as a renewable energy resource. Renew. Sustain. Energy Rev., 34: 98–109 (12 pages).

Carballo, J.; Land, L.S.; Miser, D.E., (1987). Holocene dolomitization of supratidal sediments by active tidal pumping, sugarloaf key, Florida. J. Sediment. Res., 57(1): 153–165 **(13 pages).**

Cheng, C.; Zhaomin, W.; Luyu, S.; Chengyan, L., (2022). Modeling the thermal processes within the ice shelf–ocean boundary current underlain by strong pycnocline underneath a cold-water ice shelf using a 2.5-dimensional vertical slice model. Ocean Modelling. 177: 102079 **(19 pages).**

Coogan; J.; Dzwonkowski; B.; Lehrter; J., (2019). Effects of coastal upwelling and downwelling on hydrographic variability and dissolved oxygen in mobile Bay. J. Geophys. Res. Ocean., 124(2):791–806 **(16 pages).**

Cucco, A.; Giovanni, Q.; Antonio, O.; Leopoldo, F.; Alberto, R.; Matteo, S.; Costanza, T.; Roberto S., (2016). Hydrodynamic modelling of coastal seas: the role of tidal dynamics in the Messina Strait, Western Mediterranean Sea. Nat. Hazards Earth Syst. Sci., 16(7): 1553–1569 **(17 pages).**

DHI, (2017). MIKE 21 Dan MIKE 3 flow model FM. 1–64 **(64 pages).**

Ding; Y.; Bao, X.; Yu, H.; Kuang, L., (2012). A numerical study of the barotropic tides and tidal energy distribution in the Indonesian seas with the assimilated finite volume coastal ocean model. Ocean Dyn., 62(4): 515–532 **(18 pages).**

Du, Z.; Yu Q.; Peng, Y.; Wang, L.; Lin, H.; Wang, Y., Gao, S., (2022). The formation of coastal turbidity maximum by tidal pumping in well-mixed inner shelves. J. Geophys. Res. Ocean., 127(4): 1-29 **(29 pages).**

Fauziyah, A.; Setiawan, A.; Agustriani, F.; Rozirwan; Melki; Ningsih, E.N.; Ulqodry, T.Z., (2022). Distribution pattern of potential fishing zones in the Bangka Strait waters: An application of the remote sensing technique. Egypt. J. Remote Sens. Space Sci., 25(1): 257–265 **(9 pages).**

Fourniotis, N.T., (2024). Effect of internal waves on the hydrodynamics of a Mediterranean Sea strait. J. Mar. Sci. Eng., 12(4): 1–19 **(19 pages).**

Fu, M.; Lin, J.; Zhang, P.; Luo, W.; Zhang, J., (2023). Tide drives nutrients variation and exchange flux in the semi-enclosed Shuidong Bay coastal water in winter, South China Sea. Ocean Coast. Manage., 242: 106710 **(15 pages).**

Gonzalez; N. M.; Waldman, R.; Sannino, G.; Giordani, H.; Somot, S., (2023). Understanding tidal mixing at the Strait of Gibraltar: A high-resolution model approach. Prog. Oceanogr., 212: 102980 **(15 pages)**.

Hananto, P.W.H.; Prananda, R.R., (2020). Success story to eradicate the marine pollution in international strait or strait for international trade. Crepido, 2(2): 97–110 **(14 pages).**

Hatayama, T.; Awaji, T.; Akitomo, K., (1996). Tidal currents in the Indonesian seas and their effect on transport and mixing. J. Geophys. Res., 101: 12353-12373 **(21 pages).**

Hazim; S.; Salih, A.; Taha Janan, M.; Ouatouati, A. El; Ghennioui, A., (2021). Marine current energy assessment and the hydrodynamic design of the hydrokinetic turbine for the Moroccan Mediterranean Coast. Energy Explor. Exploit., 39(3): 717–737 **(21 pages)**.

He, J.; Mahadevan, A., (2021). How the source depth of coastal upwelling relates to stratification and wind. J. Geophys. Res.: Oceans, 126(12): 1–19 **(19 pages).**

Hosseini, S. T.; Stanev, E.; Pein, J.; Valle-Levinson, A.; Schrum, C., (2023). Longitudinal and lateral circulation and tidal impacts in salt-plug estuaries. Front. Mar. Sci., 10: 1–20 **(20 pages).**

Huang; Y.; Li; G., (2024). Research on tidal energy prediction method based on improved time-varying filter-empirical mode decomposition and confluent double-stream neural network. Ocean Eng., 312(P3): 1-20 **(20 pages)**.

Jeon, W.H.; Lee, S.H.; Moon, H.S.; Kim, Y.; Chang, S.W.; Hwang, S., (2024). Impacts of pumping on the spatiotemporal dynamics of a fresh-saline water mixing zone in a coastal lagoon-aquifer system. J. Hydrol.: Reg. Stud., 51: 101657 **(17 pages).**

Johnston, T.M.S.; Colin, P.L., (2022). Upwelling and downwelling driven by the North Equatorial Countercurrent and internal waves at Hatohobei Island and Helen Reef, Palau. J. Geophys.

Res.: Oceans, 127(2): 1–18 **(18 pages).**

Kersten, M.; Bigalke, M.; Sieber, M.; Wiggenhauser, M., (2022). Cadmium isotope fractionation in an intertidal soil induced by tidal pumping. Environ. Adv., 8: 100182 **(7 pages).**

Kurniawan, A.; Khakhim, N.; Hardjo, K.S.; Santoso, A.I.; Pranowo, W.S., (2021). Constructing an imaginary wall in the ocean: A technical cartography study on the delimitation of maritime boundaries in the provinces of South Sumatra and Bangka Belitung Islands based on GIS. ASEAN J. Sci. Technol. Dev., 38(2): 51–58 **(8 pages).**

Kusumawardani, N.; Djamaluddin, R.; Angmalisang, P.A.; Manu, L.; Pelle, W.E., (2024). Characteristics of sea surface current during the second transitional monsoon in the Bangka Strait, North Sulawesi, Indonesia. Aquatic Sci. Manage., 12(1): 7–13 **(7 pages).**

Leclercq; T.; Chavanne; C.; Larouche; P., (2024). Upwellings and downwellings on the edge of the Gaspé Current: Observations and processes. Reg. Stud. Mar. Sci., 69:1-12 **(12 pages).**

Li, H.; Guo, P.; Liu, G.; Suo, A.; Zhou, W.; Yue, W.; Jiao, M.; Zhang, L., (2024). Numerical study of the upwelling and downwelling effects of artificial reefs along tidal cycles in the Pearl River Estuary. J. Environ. Manage., 365:1-15 **(15 pages**)

Liu, Y.; Jiao, J.J.; Liang, W.; Luo, X., (2017). Tidal pumping-induced nutrients dynamics and biogeochemical implications in an intertidal aquifer. J. Geophys. Res.: Biogeosci., 122(12): 3322–3342 **(21 pages).**

Lorente, P.; Piedracoba, S.; Montero, P.; Sotillo, M.G.; Ruiz, M.I.; Álvarez-Fanjul, E., (2020). Comparative analysis of summer upwelling and downwelling events in NW Spain: A model-observations approach. Remote Sens., 12(17): 1-32 **(32 pages).**

Malik, K.; Pranowo, W.S.; Sukoco, N.B.; Adrianto, D.; Setiyadi, J.; Handoko, D., (2023). Hydrodynamic characteristics of the Lombok Strait during the 2022 west monsoon peak and estimation of ocean current power generation potential. Comput. Exp. Res. Mater. Renew. Energy. 6(2): 72-88 **(16 pages).**

Martín, J.; Alonso, G.; Dragani, W.; Meyerjürgens, J.; Giesecke, R.; Cucco, A.; Fenco, H., (2023). General circulation and tidal wave propagation along the Beagle Channel. J. Mar. Syst., 240: 103889 **(15 pages).**

Mustikasari, E.; Dewi, L.C.; Heriati, A.; Pranowo, W.S., (2015). Pemodelan pola arus barotropik musiman 3 dimensi (3D) untuk mensimulasikan fenomena upwelling di perairan Indonesia. J. Segara, 11(1): 25-35 **(21 pages).**

Nakanowatari, T.; Nakamura, T.; Mitsudera, H.; Nishioka, J.; Kuroda, H.; Uchimoto, K., (2021). Interannual to decadal variability of phosphate in the Oyashio region: Roles of wind-driven ocean current and tidally induced vertical mixing in the Sea of Okhotsk. Prog. Oceanogr., 197: 102615 **(16 pages).**

Neill, P.; Hashemi, R.M., (2018). Fundamentals of ocean renewable energy: Generating Electricity from the Sea. Elsevier.

Nugroho; D.; Koch-Larrouy, A.; Gaspar, P.; Lyard, F.; Reffray, G.; Tranchant, B., (2018). Modelling explicit tides in the Indonesian seas: An important process for surface sea water properties. Mar. Pollut. Bull., 131: 7–18 **(12 pages)**.

Orhan; K.; Mayerle, R., (2020). Potential hydrodynamic impacts and performances of commercial-scale turbine arrays in the Strait of Larantuka, Indonesia. J. Mar. Sci. Eng., 8(3): 0223 **(16 pages).**

Pamungkas, A.; Husrin, S., (2020). Pemodelan sebaran sedimen tersuspensi dampak penambangan timah di perairan Bangka. J. Ilmu Teknol. Kelautan Trop., 12(2): 353–368 **(16 pages).**

Podymov, O.I.; Ocherednik, V.V.; Silvestrova, K.P.; Zatsepin, A.G., (2023). Upwellings and downwellings caused by mesoscale water dynamics in the coastal zone of northeastern Black Sea. J. Mar. Sci. Eng., 11(8): 1628 **(17 pages).**

Pranowo, W.S.; Puspita, C.D.; Bramawanto, R.; Adi, R.A.; Kusumawardani, A.R.T.D., (2014). Dinamika arus dalam mendukung perikanan budidaya laut di Teluk Bone. Harpodon Borneo, 7(2): 135 -152 **(18 pages).**

Rahuna; D.; Erwandi; Kasharjanto, A.; Suyanto, E. M.; Mintarso, C. S. J., (2023). Experimental study on hydrodynamic aspects of turbine which convert hydrokinetic and potential coastal wave energy. IOP Conf. Ser.: Earth Environ. Sci., 1166(1): 012021 **(8 pages)**.

Sabhan; Pranowo, W.S.; Purba, M.; Koropitan, A.F., (2020). Model perpindahan vertikal massa air oleh interaksi arus dan topografi di Teluk Palu. Positron, 10(1): 42–51 **(10 pages).**

Sánchez-Garrido; J. C.; Naranjo, C.; Macías, D.; García-Lafuente, J.; Oguz, T., (2015). Modeling the impact of tidal flows on the biological productivity of the Alboran Sea. J. Geophys. Res. Ocean., 120(11): 7329–7345 (17 pages).

Smith, M.J.D., (2021). Statistical Analysis Handbook: A comprehensive handbook of statistical concepts, techniques and software tools. The Winchelsea Press.

Song, Y.; Haidvogel, D., (1994). A semi-implicit ocean circulation model using a generalized topography-following coordinate system. J. Comp. Phys., 115(1): 228–244 **(17 pages)**.

Stevens; C. L.; Smith; M. J., (2016). Turbulent mixing in a stratified estuarine tidal channel: Hikapu Reach, Pelorus Sound, New Zealand. N. Z. J. Mar. Freshw. Res., 50(4): 485–505 **(21 pages)**.

Tiatama; S. H.; Atmodjo, W.; Widiaratih, R., (2024). Analisis keterkaitan fenomena supermoon terhadap komponen pasang surut di perairan Semarang, Jawa Tengah. Indones. J. Oceanogr., 6(2): 114–120 (7 pages).

Trautman, N.; Walter, R.K., (2021). Seasonal variability of upwelling and downwelling surface current patterns in a small coastal embayment. Cont. Shelf Res., 226: 104490 **(12 pages).**

Wu, L., (2021). Effects of tides and pumping on seawater intrusion in coastal aquifers. 7th Int. Conf. Hydraul. Civ. Eng. Smart Water Conserv. Intell. Disaster Reduct. Forum, ICHCE and SWIDR 2021, 1795–1800 **(6 pages)**.

Xiao, C.; Fan, W.; Qiang, Y.; Xu, Z.; Pan, Y.; Chen, Y., (2018). A tidal pump for artificial downwelling: Theory and experiment. Ocean Eng., 151: 93–104 **(12 pages).**

Xu, Y.; Liu, X.; Zhou, F.; Chen, X.; Ye, R.; Chen, D., (2023). Tide-induced upwelling and its three-dimensional balance of the vertical component of vorticity in the wider area of the Bohai Strait. J. Mar. Sci. Eng., 11(9): 1-20 **(20 pages).**

Xu; H.; Wang; G.; Huang; Z.; Su; Y.; Bai; Y.; Zhang; J., (2023). Hydrodynamic interactions between tide and runoff in the Luanhe Estuary in Bohai Sea, China: From aquaculture reclamation to restoration. Ocean Coast. Manage., 239: 1-18 **(18 pages)**.

Yasra, E.; Pranowo, W.S.; Subardjo, P.; Ismunarti, D.H.; Sukoco, N.B., (2022). Eksperimen numerik hidrodinamika 3-dimensi terhadap sistem diskritisasi hybrid dan sigma perairan Selat Capalulu Maluku Utara. J. Chart Datum. 8(1): 1–14 **(14 pages).**

Yin; M.; Cao; H.; Zhao; W.; Wang; T.; Huang; W.; Cai; M., (2022). Tide-driven microplastics transport in an elongated semi-closed bay: A case study in Xiangshan Bay, China. Sci. Total Environ., 846: 157374 **(14 pages)**.

Yu; Q.; Wang, Y.; Gao, J.; Gao, S.; Flemming, B., (2014). Turbidity maximum formation in a well-mixed macrotidal estuary: The role of tidal pumping. J. Geophys. Res. Ocean., 119(11): 7705–7724 (20 pages).

Zamani, B.; Koch, M., (2020). Comparison between two hydrodynamic models in simulating physical processes of a reservoir with complex morphology: Maroon Reservoir. Water. 12(3): 1-24 **(24 pages).**

Zhao; Y.; Deng; Z.; Yu; T.; Wang; H., (2019). Numerical Study on Tidal Mixing in the Bohai Sea. Mar. Geod., 42(1): 46–63 **(18 pages).**

Zhao, C.; Daewel, U.; Schrum, C., (2019). Tidal impacts on primary production in the North Sea. Earth Syst. Dynam., 10(2): 287–317 **(31 pages).**

Zhao, F.L.; Qiu, B.Y.; Wang, H.J.; Yan, T.X., (2023). Energy saving based on a multi-objective optimization model of the tidal pumping station along the coastal area. J. Clean. Prod., 421: 138513 **(20 pages).**

Zhou, X.; Zhu, G.; Hu, S. (2020). Influence of tides on mass transport in the Bransfield Strait and the adjacent areas, Antarctic. Polar Sci., 23: 1-12 **(12 pages).**

Zou; T.; Gu; Y.; Liu; H.; Lin; Y.; Zhang; L.; Zhang; Y., (2024). High-resolution 3D hydrodynamic modeling and comprehensive assessment of tidal current energy resources. Ocean Eng., 313(P2): 1-16 **(16 pages)**.

Zubir, Z., (2015). Peranan Selat Bangka sebagai pintu gerbang dunia maritim Kota Palembang. J. Penelitian Sejarah dan Budaya. 1(2): 248–263 **(16 pages).**

AUTHOR (S) BIOSKETCHES

Pranowo, W.S., Ph.D., Adjunct Professor, [1]Study program of Oceanography, Indonesia Naval Postgraduate Military Service School (STTAL), Ganesha Street No. 1, West Kelapa Gading, Jakarta, Indonesia. [2]Research Center for Climate and Atmosphere (BRIN), B.J. Habibie Building Science and Technological Park, South Tangerang City, Banten, Indonesia. [3]Korea-Indonesia Marine Technology Cooperation and Research Center (MTCRC), Jakarta, Indonesia
- Email: *widodo.pranowo@gmail.com*
- ORCID: 0000-0002-5798-4181
- Web of Science ResearcherID: P-8252-2017
- Scopus Author ID: 24802605300
- Homepage: https://sttal.ac.id/direktorat/pasca-sarjana/oceanography/

Malik, K., B.Eng., Lieutenant Junior Grade, [1]Study program of Oceanography, Indonesia Naval Postgraduate Military Service School (STTAL), Ganesha Street No. 1, West Kelapa Gading, Jakarta, Indonesia. [2]Hydro-Oceanography Center, Indonesian Navy, Jl. Pantai Kuta V No. 1, East Ancol, North Jakarta.
- Email: *Kurnia.malik@gmail.com*
- ORCID: 0009-0001-4243-1672
- Web of Science ResearcherID: NA
- Scopus Author ID: 59278796900
- Homepage: https://sttal.ac.id/direktorat/pasca-sarjana/oceanography/

Adrianto, D., Ph.D., Captain. [1]Hydro-Oceanography Center, Indonesian Navy, Jl. Pantai Kuta V No. 1, East Ancol, North Jakarta. 2Study program of Oceanography, Indonesia Naval Postgraduate Military Service School (STTAL), Ganesha Street No. 1, West Kelapa Gading, Jakarta, Indonesia.
- Email: *aqilaadrianto@gmail.com*
- ORCID: 0000-0001-5098-2143
- Web of Science ResearcherID: NA
- Scopus Author ID: 57203358477
- Homepage: https://sttal.ac.id/direktorat/pasca-sarjana/oceanography/

Kurniawan A., M.Sc., [1]Coastal and Watershed Management Master's Study Program, Faculty of Geography, Universitas Gadjah Mada, Jl. Kaliurang, Sekip Utara, Bulaksumur Sinduadi Sleman, Sendowo, Sinduadi, Kec. Mlati, Kabupaten Sleman, Daerah Istimewa Yogyakarta, Indonesia. [2]Study program of Oceanography, Indonesia Naval Postgraduate Military Service School (STTAL), Ganesha Street No. 1, West Kelapa Gading, Jakarta, Indonesia.
- Email: *agung.kurniawan.16@mail.ugm.ac.id*
- ORCID: 0000-0002-2441-8706
- Web of Science ResearcherID: NA
- Scopus Author ID: 57372228100
- Homepage: https://sttal.ac.id/direktorat/pasca-sarjana/oceanography/

HOW TO CITE THIS ARTICLE

Widodo, S.P.; Malik, K.; Adrianto, D.; Kurnaiwan, A., (2025). Hydrodynamic simulation experiment of tidal pump in strait waters. Global J. Environ. Sci. Manage., 11(2): 593-608.

DOI: 10.22034/gjesm.2025.02.13

URL: https://www.gjesm.net/article_719921.html